

# Synthesis and Properties of Side Chain Ferroelectric Liquid Crystalline Polyacetylene Derivatives

X. M. Dai, H. Goto, K. Akagi\*, H. Shirakawa

Institute of Materials Science, University of Tsukuba, Tsukuba, Ibaraki 305-8573, Japan

Fax: +81-298-55-7440, akagi@ims.tsukuba.ac.jp

## Abstract

Novel liquid crystalline (LC) polyacetylene derivatives were synthesized to develop advanced LC conducting polymers with an ability of quick response to an electric field used as an external force. In practice, we synthesized ferroelectric LC conducting polymers by introducing fluorine-containing chiral LC groups into side chains of polyacetylenes. Phase transition behaviors of these polymers were examined by differential scanning calorimeter and polarizing optical microscope. Mesophases as well as higher order structures were evaluated with X-ray diffraction measurements. Two of the polymers synthesized showed chiral nematic (N\*) and chiral smectic C (S<sub>C</sub>\*) phases in the heating and cooling processes. Observation of the S<sub>C</sub>\* phase allows us to expect that the polymer should exhibit the ferroelectricity.

Keywords: Polyacetylene and derivatives, Liquid crystalline phase transitions, Chirality, Ferroelectricity.

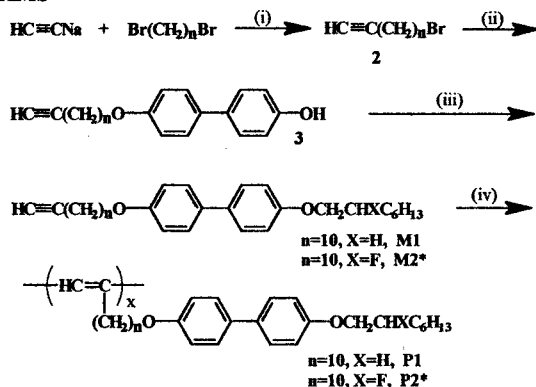
## 1. INTRODUCTION

Conjugated polymers with liquid crystalline (LC) groups in side chains have been drawing current interests from view points of multifunctional electrical and optical materials [1-3]. Spontaneous orientation and externally forced alignment of the LC side chains enabled us to control electrical and optical properties as well as their anisotropies [4-6]. When an electric field is employed as an external force, ferroelectric LC (FLC) side chains should be more desirable than ordinary LC ones, because the former is expected to respond more quickly to the electric field owing to its spontaneous polarization than the latter. In other words, the spontaneous polarization formed in chiral smectic C (S<sub>C</sub>\*) phase is responsible for the ferroelectric liquid crystallinity. Recently, we synthesized polyacetylene derivatives substituted with chiroptical LC groups, and confirmed a formation of the S<sub>C</sub>\* phase attributable to the ferroelectric liquid crystallinity [7,8], although the temperature region of the liquid crystalline phase was as narrow as 5 degrees. Here, we synthesized advanced FLC polyacetylene derivatives with thermally more stable S<sub>C</sub>\* phase, by introducing fluorine-containing chiral LC groups into side chains.

## 2. EXPERIMENTAL

**Techniques:** All <sup>1</sup>H-NMR and <sup>13</sup>C-NMR spectra were measured with a BRUKER 500 MHz FT-NMR spectrometer. CDCl<sub>3</sub> was used as a deuteration solvent and TMS was used as an internal standard. Infrared spectroscopic measurement was carried out with a Jasco FT-IR 550 spectrometer using KBr method. Phase transition temperatures were determined using a Perkin-Elmer differential scanning calorimeter (DSC 7) apparatus at a constant heating/cooling rate of 10°C/min and optical texture observation was performed using a Nikon polarizing microscope equipped with a Linkam

## THMS



(i). DMF; (ii). K<sub>2</sub>CO<sub>3</sub>, 4,4'-biphenyldiol, butanone;  
 (iii). azodicarboxylic acid diethyl ester (DEAD), triphenylphosphine (TPP), (S) - C<sub>6</sub>H<sub>13</sub>CHXOH (X=H, F), THF; (iv). [Rh(NBD)Cl]<sub>2</sub>, NEt<sub>3</sub>, THF.

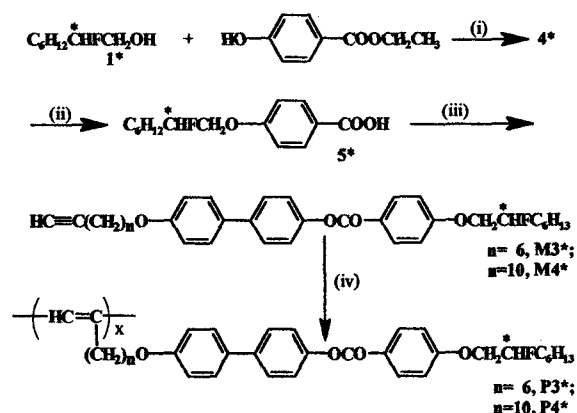
Scheme 1 Synthesis of monomers (M1, M2\*) and polymers (P1, P2\*)

600 hot stage. Purities of intermediates and final compounds were checked by HPLC analysis. Molecular weights of polymers were determined by gel permeation chromatography (GPC) with a Shodex A-80M column and a Jasco HPLC 870-UV detector, and THF was used as a solvent. XRD measurements were performed with a Rigaku D-3F diffractometer, in which X-ray power and scanning rate were set at 200 mW and 5 deg/min, respectively.

**Materials:** The chiral alcohol (S)-(-)-2-fluorooctanol (1\*) was prepared according to the method reported by Nohira et al [9], in which (R)-(+)-1,2-epoxyoctane was reacted with pyridinium poly (hydrogen fluoride) in ether.

The synthetic routes of monomers and polymers

are



(i). DEAD, TPP, THF; (ii). NaOH, CH<sub>3</sub>OH, HCl; (iii). compound *N,N'*-dicyclohexylcarbodiimide (DCC), 4-(dimethylamino)pyridine (DMAP), CH<sub>2</sub>Cl<sub>2</sub>; (iv). [Rh(NBD)Cl]<sub>2</sub>, NEt<sub>3</sub>, THF.

Scheme 2 Synthesis of monomers (M3\* and M4\*) and polymer (P3\* and P4\*)

shown in Schemes 1 and 2. 12-Bromo-1-dodecyne (**2**) was prepared by reacting sodium acetylide with 1,10-dibromodecane in DMF. 4-Hydroxy-4'-(11-dodecyloxy)biphenyl (**3**) was obtained by reacting compound **2** with 4,4'-dihydroxybiphenyl in the presence of K<sub>2</sub>CO<sub>3</sub>. 4-Octyloxy-4'-(11-dodecyloxy)biphenyl (**M1**) and 4-[(*S*)-2-Fluorooctyloxy]-4'-(11-dodecyloxy)biphenyl (**M2\***) were obtained by coupling compound **3** with *n*-octanol and compound **3** with compound **1\***, respectively, using the Mitsunobu reaction in THF [10, 11]. In Scheme 2, ethyl 4-[(*S*)-2-fluorooctyloxy]benzoate (**4\***) was synthesized by coupling compound **1\*** with ethyl *p*-hydroxybenzoate under the same condition as that of the synthesis of compound **M2\***. The basic hydrolysis of compound **4\*** with KOH in a solution of methanol and water, led to the formation of 4-[(*S*)-2-fluorooctyloxy]benzoic acid (**5\***). Besides, the esterification of compound **3** with compound **5\*** in the presence of dicyclohexylcarbodiimide (DCC) and 4-dimethylaminopyridine (DMAP) gave rise to the formation of 4-[4-[(*S*)-2-fluorooctyloxy]benzoyl]-4'-(9-octyloxy)biphenyl (**M3\***) and 4-[4-[(*S*)-2-fluorooctyloxy]benzoyl]-4'-(11-dodecyloxy)biphenyl

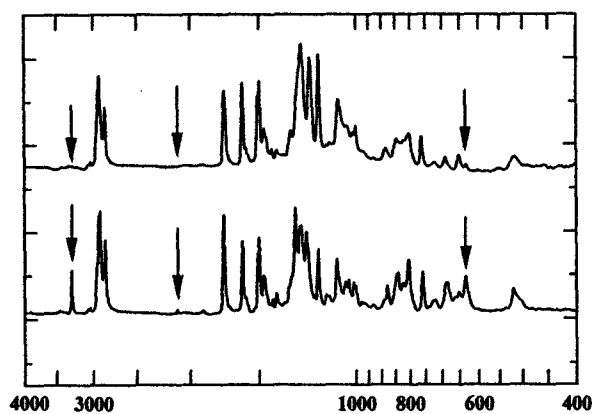


Fig. 1 IR spectra of P4\* (upper) and M4\* (lower)

(M4\*).

The LC groups of acetylene monomers, **M1** and **M2\***, are composed of a biphenyl moiety as a mesogenic core, and a decamethylene chain as a spacer, and terminal moieties that are *n*-octyloxy and (*S*)-2-fluorooctyloxy groups, respectively. Meanwhile, the LC groups of acetylene monomer, **M3\*** and **M4\***, are composed of a biphenyl moiety linked with a phenyl moiety via an ester linkage as a mesogenic core, a decamethylene or a hexamethylene chain as a spacer, and (*S*)-2-fluorooctyloxy group as a terminal moiety.

Polymerizations of the acetylene monomers (**M1**, **M2\***, **M3\*** and **M4\***) were carried out using rhodium catalyst, [Rh(NBD)Cl]<sub>2</sub>-NEt<sub>3</sub>, where NBD stands for 2,5-norbornadiene. All polymers synthesized (**P1**, **P2\***, **P3\*** and **P4\***) were fusible and soluble in common organic solvents including tetrahydrofuran (THF).

### 3. RESULTS AND DISCUSSION

Number-average ( $M_n$ ) and weight-average ( $M_w$ ) molecular weights of **P1** were  $9.1 \times 10^3$  and  $1.4 \times 10^4$ , respectively. The  $M_n$  and  $M_w$  of **P2\*** were  $1.5 \times 10^4$  and  $4.4 \times 10^4$ , respectively. The  $M_n$  and  $M_w$  of **P3\*** were  $1.1 \times 10^4$  and  $2.7 \times 10^4$ , respectively, and those of **P4\*** were  $1.1 \times 10^4$  and  $1.8 \times 10^4$ , respectively. Representative IR spectra of the monomer and polymer, **M4\*** and **P4\*** are shown in Fig. 1. It is found that the three typical absorption peaks of acetylenic moiety in the

Table 1 Phase transition temperatures of LC polyacetylene derivatives

Polymer	Phase transition temperature (°C)	
	Heating	Cooling
<b>P1</b>	G 144 S <sub>A</sub> 164 I	I 158 S <sub>A</sub> —S <sub>X</sub> 142 G
<b>P2*</b>	G 121 S <sub>A</sub> 149 I	I 144 S <sub>A</sub> —S <sub>X</sub> 117 G
<b>P3*</b>	G 121 S <sub>C</sub> * 168 N* 217 I	I 214 N* 158 S <sub>C</sub> * 115 G
<b>P4*</b>	G 135 S <sub>C</sub> * 182 N* 217 I	I 213 N* 177 S <sub>C</sub> * 126 S <sub>X</sub> 105 G

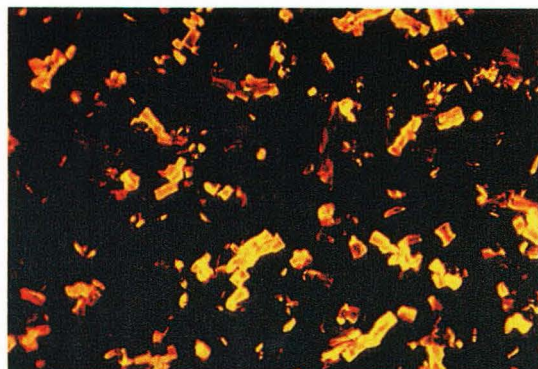
I: isotropic, N\*: chiral nematic, S<sub>C</sub>\*: chiral smectic C, S<sub>X</sub>: unidentified smectic phases, G: glassy state.

monomer disappeared after the polymerization.  $^1\text{H}$ -NMR measurements showed that the proton signal at 1.9 ppm of the acetylenic moiety ( $\text{HC}\equiv\text{C}-$ ) in the monomer (e.g.,  $\text{M4}^*$ ) shifted to the lower magnetic field after the polymerization, and it was merged into the signals of the aromatic rings (6~7 ppm) of the side chain. Similarly, the  $^{13}\text{C}$ -NMR measurements showed that the signals at 67 and 85 ppm of the acetylenic carbons ( $\text{HC}\equiv\text{C}-$ ) in the monomer (e.g.,  $\text{M4}^*$ ) shifted to the lower magnetic field after the polymerization, and they were merged

into the signals of the aromatic carbons (120~140 ppm) of the side chain. These results suggest that the acetylenic moiety has changed into the olefinic moiety ( $-\text{HC}=\text{C}<$ ) after the polymerization. Unfortunately, however, the chemical shifts of the olefinic proton and carbons in the polymer are very close to those of the aromatic phenyl and/or biphenyl moieties in the LC side chain, and therefore they were unambiguously identified.

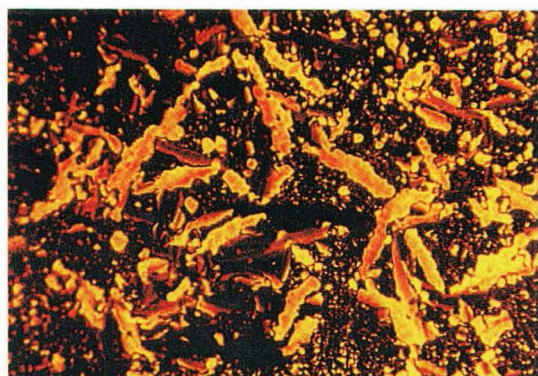
The phase transition temperatures are summarized in Table 1. The acetylene monomers,  $\text{M1}$  and  $\text{M2}^*$ , showed no mesophase. The precursor  $5^*$  exhibited enantiotropic chiral nematic ( $\text{N}^*$ ) and smectic ( $\text{S}$ ) phases. This is probably due to a formation of hydrogen bonding dimer of  $5^*$ .  $\text{M3}^*$  showed enantiotropic  $\text{N}^*$  and  $\text{S}_\text{C}^*$  phases. On cooling from the isotropic phase,  $\text{M4}^*$  showed  $\text{N}^*$  and  $\text{S}_\text{C}^*$  phases and two unidentified higher order smectic phases.

All polymers exhibited mesophases.  $\text{P1}$  showed smectic A ( $\text{S}_\text{A}$ ) and higher order smectic phases, and  $\text{P2}^*$  showed  $\text{S}_\text{A}$  and  $\text{S}_\text{X}^*$  phases on the cooling process. The optical textures of  $\text{P1}$  and  $\text{P2}^*$  are shown in Figs. 2 and 3, respectively. XRD analysis suggested that  $\text{P2}^*$  may exhibit a higher order smectic phase, but not  $\text{S}_\text{C}^*$  one. On the other hand,  $\text{P3}^*$  showed enantiotropic  $\text{N}^*$  and  $\text{S}_\text{C}^*$  phases.  $\text{P4}^*$  showed  $\text{S}_\text{C}^*$  and  $\text{N}^*$  phases on the heating process, and  $\text{N}^*$ ,  $\text{S}_\text{C}^*$  and  $\text{S}_\text{X}$  phases in the cooling one. The typical optical textures of  $\text{P4}^*$  are shown in Fig. 4.

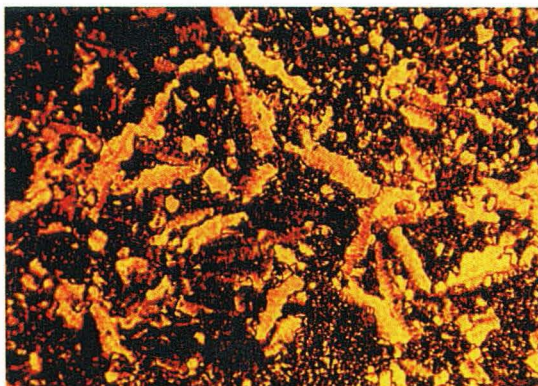


100  $\mu\text{m}$

Fig. 2 Polarizing optical micrograph of  $\text{P1}$ .  
Batonnets texture ( $\text{S}_\text{A}$ ) at 160  $^\circ\text{C}$

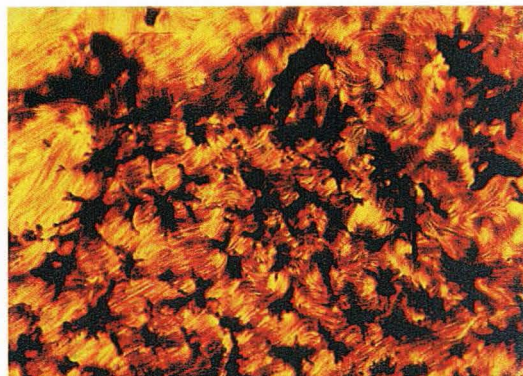


100  $\mu\text{m}$

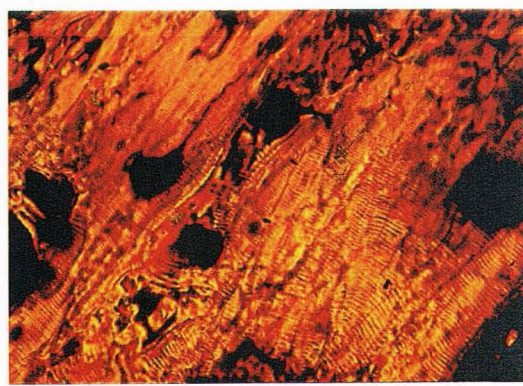


100  $\mu\text{m}$

Fig. 3 Polarizing optical micrographs of  $\text{P2}^*$ .  
Batonnets texture ( $\text{S}_\text{A}$ ) at 140  $^\circ\text{C}$  (upper);  
Striated batonnets texture ( $\text{S}_\text{X}^*$ ) at 120  $^\circ\text{C}$  (lower).



100  $\mu\text{m}$



100  $\mu\text{m}$

Fig. 4 Polarizing optical micrographs of  $\text{P4}^*$ .  
Finger-printed texture of chiral nematic ( $\text{N}^*$ ) phase at 193  $^\circ\text{C}$  (upper);  
Parabolic texture of chiral smectic C ( $\text{S}_\text{C}^*$ ) phase at 165  $^\circ\text{C}$  (lower).

Table 2 Results of XRD measurements and MM calculations of LC-substituted polyacetylene derivatives

Polymer	LC phase	Temp. (°C)	XRD		MM				Relative stability (kcal/unit)
			Interlayer distance (Å)	Inter side chain distance (Å)	One side (I) (Å)		Both side (II) (Å)		
					Interlayer distance	Inter side chain distance	Interlayer distance	Inter side chain distance	
P1	S <sub>A</sub>	—	—	—	34.7	4.6	67.5	4.4	I > II
	S <sub>X</sub>	r. t.	55.2	4.0~4.4	—	—	—	—	by 4.5
P2*	S <sub>A</sub>	—	—	—	34.8	4.5	67.4	4.3	I > II
	S <sub>X</sub> *	r. t.	52.1	4.1~4.4	—	—	—	—	by 4.4
	N*	190	38.3	4.6	40.6	4.4	79.9	4.2	I > II
P4*	S <sub>C</sub> *	160	33.0	4.6	—	—	—	—	by 3.3
	S <sub>X</sub> *	120	35.4	4.5	—	—	—	—	

XRD pattern of P4\* measured in the LC phase at 190 °C gave two reflection peaks corresponding to the distances of 4.62 and 38.5 Å. At this temperature, the finger printed texture was observed in POM of P4\* (Fig. 4, upper). Such a texture is characteristic of N\* phase. This is the first result to observe N\* phase in LC conjugated polymers. When the temperature was cooled to 160 °C, the *d*-spacing of the small angle reflection decreased from 38.5 to 33.0 Å, suggesting the formation of S<sub>C</sub>\* phase. A parabolic texture of S<sub>C</sub>\* phase for P4\* was observed at this temperature (Fig. 4, lower). When the temperature was further cooled to 120 °C, the *d*-spacing of the small angle reflection increased from 33.0 to 35.4 Å and the wide angle reflection became sharp. This result suggests the formation of a tilted smectic phase.

Generally there are two possible structures for the LC-substituted polyacetylene derivatives, where the side chains are located on the one side or both sides of the main chain. They are abbreviated as "one-side" and "both-side" structures, respectively. In the case of P1, the molecular mechanics (MM) calculations showed that the *d*-spaces (interlayer distances) of the one-side and both-side structures, are 34.7 Å and 67.5 Å, respectively. XRD measurements gave a *d*-space of 55.2 Å, which is close to that of the both-side structure. All of the results are summarized in Table 2. Taking account of results of XRD measurements and MM calculations, it can be argued that P1 and P2\* polymers have the both-side structure, while P3\* and P4\* polymers the one-side structure.

Lastly, electrical conductivities of the non-oriented cast films of P1, P2\*, P3\* and P4\* after iodine doping were  $4 \times 10^{-7}$ ,  $7 \times 10^{-7}$ ,  $5 \times 10^{-5}$  and  $2 \times 10^{-4}$  S/cm, respectively.

In conclusion, novel LC polyacetylene derivatives have been synthesized by introducing achiral LC group or chiral fluorine-containing LC group into side chains.

Two of the polymers (P3\* and P4\*) showed S<sub>C</sub>\* phase with an enantiotropic behavior, whose temperature region was sufficiently wide such as 50 degrees. It is therefore expected that these polymers should be available for ferroelectric LC conducting materials.

#### 4. ACKNOWLEDGMENTS

This work was supported by Grant-in-Aids for Scientific Research from the Ministry of Education, Culture and Science, and in part by the Akagi project of Tsukuba Advanced Research Alliance (TARA) of University of Tsukuba.

#### 5. REFERENCES

- [1] K. Akagi, H. Shirakawa, *Macromol. Symp.*, **104**, 137 (1996).
- [2] K. Akagi, H. Shirakawa, *The Polymeric Materials Encyclopedia. Synthesis, Properties and Applications*, CRC Press, 5, pp. 3669, 1996.
- [3] K. Akagi, H. Shirakawa, in D. L. Wise, et al (eds.), *Electrical and Optical Polymer Systems: Fundamentals, Methods, and Applications*, Marcel Dekker, 28, pp. 983, 1998.
- [4] S.-Y. Oh, K. Akagi, H. Shirakawa, K. Araya, *Macromolecules*, **26**, 6203, (1993).
- [5] K. Akagi, H. Goto, Y. Kadokura, H. Shirakawa, S.-Y. Oh, K. Araya, *Synth. Met.*, **69**, 13, (1995).
- [6] K. Akagi, H. Goto, H. Shirakawa, T. Nishizawa, K. Masuda, *Synth. Met.*, **69**, 33, (1995).
- [7] K. Akagi, H. Goto, H. Shirakawa, *ACS, Polym. Prepr.*, **37** 62 (1996)
- [8] K. Akagi, H. Goto, H. Shirakawa, *Synth. Met.*, **84**, 313, (1997).
- [9] H. Nohira, S. Nagamura and M. Kamei, *Mol. Cryst. Liq. Cryst.*, **180B**, 379 (1990).
- [10] O. Mitsunobu and M. Yamada, *Bull. Chem. Soc. Jpn.* **40**, 2380 (1967).
- [11] S. Bittner and Y. Assaf, *Chem. Indust.* **15**, 281 (1975).